ROBUST STATE ESTIMATION METHOD OF DISTRIBUTION NETWORK FOR STOCHASTIC VARIABLES WITH DYNAMIC INTERVAL VALUES

Li Xin,* Wu Jiekang,** Zeng Shunqi,* and Cai Jinjian**

Abstract

The uncertainties in measurement make the estimation accuracy of traditional methods difficult to meet the dispatching requirements of distribution systems. At the same time, the measurement system often has bad data during the acquisition and transmission process, which seriously affects the accuracy of state estimation. The method in this paper is used to improve the influence of the state estimation on measurement uncertainty and bad data, and improve the robustness and accuracy of estimation. Interval analysis method is used to describe the measurement problem with uncertainties, the interval constraint model of state variables in distribution network is established, and the feasible region of state variables is obtained using linear programming method. Based on the measurement uncertainty theory, a robust state estimation optimization model with the highest measurement point accuracy as the objective function is established. The precise value of the state estimation is solved by the interior point method. With the feasible region of state variables as constraints and the median value of the interval as the initial value, it is unnecessary to take the calculation results of power flow as the initial value, thus reducing the scope of solving state variables and reducing the amount of calculation. Compared with the traditional weighted least square, this method has a significant improvement in accuracy and resistance. The feasibility and effectiveness of this method are verified by IEEE30 and IEEE118 systems.

Key Words

Distribution network, robust state estimation, dynamic interval analysis, interval value constraint, linear programming, interior point method

* Guangzhou Power Supply Bureau of Guangdong Power Grid Co., Ltd., China

** School of Automation, Guangdong University of Technology, China; e-mail: wujiekang@163.com

Corresponding author: Wu Jiekang

Recommended by Prof. Yao Xu

(DOI: 10.2316/J.2022.203-0393)

1. Introduction

Using state estimation [1]–[10] can evaluate the operation situation of the buses in power system and the state value of voltage and power through observable information, so as to provide reliable and real data information for optimal power flow, reactive power optimization, and other applications. At the same time, the redundancy of the real-time measurement system is used to improve the system accuracy, and the bad data detection and identification are used to automatically eliminate the error information caused by random interference [2].

Distribution network multi-source data involve a huge amount of information, mainly considering the following three real-time data, including Supervisory Control And Data Acquisition (SCADA), phasor measurement unit (PMU), and advanced measurement system. At present, the state estimation method based on weighted least square (WLS) [3] is widely used, but it is easy to be affected by bad data, resulting in poor robustness. Many experts and scholars have made great efforts in the field of the state estimation and achieved a lot of fruitful results. The latest development in the field of the state estimation is based on the estimation method that "the state approved by the most measurement points is the most reasonable state" [4]–[7].

Based on the theory of measurement uncertainty, under the premise of determining the error distribution, the uncertainty measure can give the confidence interval through quantitative evaluation method and study the robustness of the state estimation algorithm in the form of interval. When the state estimation value of a measuring point is in the range of the measured value, the measured point is considered to be effective. The more the effective states measured by a certain system, the closer the state estimation results is to the real operation situation, so as to improve the anti-interference ability of bad data [8].

It is difficult and complex to carry out the state estimation considering the influence of uncertainty factors. There are many research results in this work. For example, based on the definition of normal measurement point, the

evaluation function of measurement point is established, and in the state estimation model with the maximum normal rate of measurement point as the objective function, the state estimation result is not easily affected by bad data and has good robustness [4]–[6]; on this basis, by checking the abnormal points and filtering the normal points, higher accuracy of the state estimation is obtained [7]. Based on the uncertainty measurement theory, taking the maximum normal rate and the minimum deviation degree as the objective function of the state estimation, a multi-objective programming model of the state estimation is proposed, which has the advantages of small sample estimation, adaptability to measurement data, strong robustness, and easy solution point [8]–[10].

As it is impossible to obtain the true values of the grid parameters, the upper and lower limits may be known in most cases [11]. The interval analysis method [12] is applied in the state estimation to analyse uncertainty problems. For example, using the form of interval to describe the uncertainty of measurement data, establishing the three-phase interval state estimation model of active distribution network, and solving by linear programming, the state estimation results also show the form of interval [13], which has certain advantages in estimation accuracy and operation efficiency. When considering uncertainty, interval analysis can effectively optimize the configuration of micro PMUs and smart meters while ensuring the accuracy of the state estimation in [14]. Considering the conservatism and correlation of interval operation, the interval state estimation model of distribution network is established by combining interval mathematics with affine mathematics, which improves the reliability of estimation results [15]; for the uncertainty of parameters and measurement of power grid, an interval state estimation method based on the Krawczyk operator is adopted to deal with the uncertainty problem of the parameters and measurement, and a state interval with better accuracy is obtained [16]. An interval state estimation can well deal with the uncertainty of distributed power generation and line parameters and obtain strict boundaries of state variables [17], but it does not consider the problem of decreased accuracy of interval estimation under the influence of bad data.

In solving process, interval operation is conservative sometimes because of interval expansion. At the same time, when using linear programming method to solve the problem, the number of iterations increases with the increase of system scale. Relevant research shows that considering the actual physical numerical constraints, the solution range of state variable is wide, the maximum value of historical data based on the node can be considered as the constraint, or the dynamic interval constraint can be solved according to the measurement information, which is more in line with the actual operation of power system [18]. In terms of solving methods and analysis, other documents also give good suggestions and solutions [19].

The state estimation of distribution network is based on the power flow calculation. The stability, convergence accuracy, and calculation speed of the state estimation method of distribution network will be affected by power flow calculation method. The state estimation value is solved by taking the power flow calculation value as the initial value or referring to the power flow calculation result to give the initial value [3], [18].

This paper is organized as follows. Section 2 describes the robust model of distribution network state estimation. In Section 3, algorithm for solving the proposed model is presented more in detail. Finally, the simulation results on IEEE30 and IEEE118 are given in Section 4 followed by the conclusion in Section 5.

2. Robust Model of the State Estimation of Distribution Network

2.1 Interval Value and Feasible Region

Suppose that the total number of measuring points in a system is m and the number of state variables is $2n$. The branch power measurement obtained by SCADA system can be expressed as $[P_{ij}]$ and $[Q_{ij}]$ in the form of interval value, the nodal injection power can be expressed as $[P_i]$ and $[Q_i]$ in the form of interval value, and the nodal voltage amplitude is expressed as $[V_i]$ in the form of interval value. When the equivalent measured value z_i is a certain value, its interval value is the fluctuation interval added $\pm a\%$ to the measured value, that is, the interval is expressed as $[z_i(1-a\%), z_i(1+a\%)]$. Considering the real-time measurement and the pseudo measurement of node load power, the measurement can be expressed as follows in the interval-constrained model:

$$\boldsymbol{z} = \Big[[P_i],[Q_i],[P_{ij}],[Q_{ij}],[V_i]\Big]^{\mathrm{T}} \tag{1}$$

The amplitude and phase angle of nodal voltage are selected as the state variables to be calculated:

$$\boldsymbol{x} = [V_i, \theta_i]^{\mathrm{T}} \tag{2}$$

According to the interval analysis method, the interval constraint model can be expressed as follows:

$$\begin{cases} \underline{\boldsymbol{x}}_i = \min \boldsymbol{x}_i \\ \overline{\boldsymbol{x}}_i = \max \boldsymbol{x}_i \\ s.t\ \boldsymbol{x} \in \boldsymbol{X}(M, \underline{z}, \bar{z}) \end{cases} \tag{3}$$

where $[\underline{x}_i, \bar{x}_i]$ is the uncertainty interval of the state variable, $\underline{x}_i$ is the lower limit of the state variable, and $\bar{x}_i$ is the upper limit of the state variable. $\boldsymbol{X}(\cdot)$ represents the set of uncertain factors of state variables.

Without considering the measurement correlation, the interval constraint model of distribution network can be expressed as [13]:

$$\underline{V}_i = \min V_i, \bar{V}_i = \max V_i, \underline{\theta}_i = \min \theta_i, \bar{\theta}_i = \max \theta_i$$

$$\text{s.t.} \begin{cases} [\underline{P}_i, \bar{P}_i] = V_i \left[\sum\limits_{j=1}^{n} V_d Y_{ij} \cos(\theta_i - \theta_d) \right] \\ [\underline{Q}_i, \bar{Q}_i] = V_i \left[\sum\limits_{j=1}^{n} V_d Y_{ij} \sin(\theta_i - \theta_d) \right] \\ [\underline{P}_{i'}, \bar{P}_{i'}] = 0, [\underline{Q}_{i'}, \bar{Q}_{i'}] = 0 \\ [\underline{P}_{ik}, \bar{P}_{ik}] = V_i [V_k Y_{ik} \cos(\theta_i - \theta_k)] \\ [\underline{Q}_{ik}, \bar{Q}_{ik}] = V_i [V_k Y_{ik} \sin(\theta_i - \theta_k)] \\ [\underline{V}_i, \overline{V}_i] = V_i \end{cases} \tag{4}$$

where $\bar{V}_i$ and $\underline{V}_i$ are the upper and lower limits of the voltage amplitude at the measuring point. $\bar{\theta}_i$ and $\underline{\theta}_i$ are the upper and lower limits of the voltage phase angle of the measuring point. G_{ij} and B_{ij} are the corresponding conductance and admittance in the node admittance matrix Y_{ij}; i' is the zero injection power point in the network. $\bar{P}_{i'}$ and $\underline{P}_{i'}$ are the upper and lower limits of the active power at the zero injection point. $\bar{Q}_{i'}$ and $\underline{Q}_{i'}$ are the upper and lower limits of the reactive power at the zero injection point, respectively. The voltage amplitude V_i and phase angle θ_i on the right side of the equation are expressed in the form of interval.

2.2 Optimization Model for the State Estimation

The optimization model takes the model of interval state estimation as the feasible region of the state variables and optimizes the accurate value of the voltage of each node by measuring the evaluation function, aiming at the highest accuracy rate of the measuring point. The result of the state estimation is optimized in the interval.

2.2.1 Normal Measuring Point

For measuring points, the relative deviation of measuring points at a certain confidence level is defined as:

$$d_i = \frac{\boldsymbol{h}_i(\boldsymbol{x}) - \boldsymbol{z}_i}{\boldsymbol{U}_i} \tag{5}$$

where $\boldsymbol{h}(\cdot)$ is the measurement function of the measuring point; $\boldsymbol{z}_i$ is the measurement at node i; and $\boldsymbol{U}_i$ is the uncertainty of the measuring point corresponding to the confidence level p, which is related to the accuracy of the measuring device. If the relative deviation of measuring point i under state variable $\boldsymbol{x}$ satisfies $|d_i| \leq 1$, the measuring point is judged as normal measuring point, and if $|d_i| > 1$ it is determined as abnormal measuring point.

2.2.2 Evaluation Function of Measuring Point

According to these characteristics, the evaluation function of the measuring point is set up according to the definition of normal measuring point, which is used to judge whether the measuring point is normal or not:

$$\begin{cases} f(d_i) = \delta(d_i) + \delta(-d_i) \\ \delta(d_i) = \frac{1}{1+e^{\frac{2k}{\lambda}[d_i+(1+\frac{\lambda}{2})]}} \end{cases} \tag{6}$$

The values of parameters λ and k are determined by testing method. Generally, $\lambda = 1 \sim 5$, $k = 2 \sim 4$.

2.2.3 State Estimation Optimization Model

In the actual operation process, the state variables must satisfy the power flow constraints and other physical and numerical constraints. Therefore, to maximize the number of normal measurement points, the optimization model for the state estimation of distribution network is constructed [18]:

$$\begin{aligned} &\min \sum_{i=1}^{m} f(d_i) \\ &\text{s.t.} \quad d_i = \frac{\boldsymbol{h}_i(\boldsymbol{x}) - \boldsymbol{z}_i}{\boldsymbol{U}_i}, \forall i = 1, 2, \cdots, m \\ &\qquad \boldsymbol{g}(\boldsymbol{x}) = 0 \\ &\qquad \boldsymbol{l}(\boldsymbol{x}) \leq 0 \\ &\qquad \underline{\boldsymbol{x}} \leq \boldsymbol{x} \leq \overline{\boldsymbol{x}} \end{aligned} \tag{7}$$

where m is the number of measurement points, $\boldsymbol{g}(\boldsymbol{x}) = 0$ is the power flow constraint equation, such as the injection power constraint of zero power injection node, and $\boldsymbol{l}(\boldsymbol{x}) \leq 0$ represents other actual physical numerical constraints. $[\underline{\boldsymbol{x}}, \overline{\boldsymbol{x}}]$ is the dynamic constraint of the state variable, and the interval constraint of the state variable is obtained according to the interval constraint model.

The results of the state estimation obtained from optimization model meet not only the power flow constraints but also the feasible region of state variables, which is more in line with the reality.

2.2.4 Constraint Condition

(1) Voltage Constraint

The nodal voltage satisfies the following relationship:

$$V_s = V_t + Z_l I_l \tag{8}$$

where Z_l is the impedance between node t and node s, $Z_l = R_l + jX_l$. I_l is the current flowing from node t and node s.

(2) Current Constraint

For the connected nodes (without power injection) in the distribution network, there are p branches flowing to node k, and there are q branches flowing out of node k. According to Kirchhoff's current law, the sum I_{in} of the current flowing into node k is equal to the sum I_{out} of the current flowing out of the node, which can be expressed as follows:

$$\sum_{l=1}^{p} I_{in} - \sum_{l=p+1}^{p+q} I_{out} = 0 \tag{9}$$

(3) Branch Power Flow Constraints

The nodal injection power in distribution network should meet the following requirements:

$$\begin{cases} P_i = V_i \sum_{j \in i} V_j (G_{ij} \cos\theta_{ij} + B_{ij} \sin\theta_{ij}) \\ Q_i = V_i \sum_{j \in i} V_j (G_{ij} \sin\theta_{ij} - B_{ij} \cos\theta_{ij}) \end{cases} \tag{10}$$

where P_i and Q_i are the active power and reactive power at node i, respectively; V_i is the voltage amplitude at node i; $j \in i$ denotes the node directly connected with node i; G_{ij} and B_{ij} are the branch conductance and admittance between node i and j; θ_{ij} is the voltage phase angle difference between node i and j, $\theta_{ij} = \theta_i - \theta_j$.

(4) Branch Power Constraint

The actual transmission power of the branch should be less than its maximum transmission power:

$$S_l \le S_l^{\max} \qquad l \in [1, N_l] \tag{11}$$

where S_l and $S_l^{\max}$ are, respectively, the actual transmission power and the maximum allowable transmission power of branch l; N_l is the total number of actually connected branches of the distribution system.

3. The Solving Method

3.1 The Solving Method for Interval-Constrained Model

In this section, the linear programming method based on iterative operation is used to solve the overdetermined equations (6) with nonlinear interval constraints. It can be transformed into a linear programming problem as shown below and solved iteratively for many times. For the specific derivation steps, please refer to [13]:

$$\begin{cases} \Delta \underline{x}_i = \min \boldsymbol{a^i} \cdot \Delta \boldsymbol{z^n} \\ s.t. \begin{cases} \Delta \underline{\boldsymbol{z}}^{\boldsymbol{n}} \le \Delta \boldsymbol{z^n} \le \Delta \overline{\boldsymbol{z}}^{\boldsymbol{n}} \\ \Delta \underline{\boldsymbol{z}}^{\boldsymbol{m-n}} \le \boldsymbol{H}^{m-n}(\boldsymbol{H}^n)^{-1} \cdot \Delta \boldsymbol{z^n} \le \Delta \overline{\boldsymbol{z}}^{\boldsymbol{m-n}} \end{cases} \end{cases} \tag{12}$$

$$\begin{cases} \Delta \bar{x}_i = \max \boldsymbol{a}^i \cdot \Delta \boldsymbol{z}^n \\ s.t. \begin{cases} \Delta \underline{\boldsymbol{z}}^n \le \Delta \boldsymbol{z}^n \le \Delta \overline{\boldsymbol{z}}^n \\ \Delta \underline{\boldsymbol{z}}^{m-n} \le \boldsymbol{H}^{m-n}(\boldsymbol{H}^n)^{-1} \cdot \Delta \boldsymbol{z}^n \le \Delta \overline{\boldsymbol{z}}^{m-n} \end{cases} \end{cases} \tag{13}$$

where $\boldsymbol{H}$ is the Jacobian matrix corresponding to the measurement function $\boldsymbol{h}(\boldsymbol{x})$, $\boldsymbol{a}^i$ is corresponding to row i in the matrix $\boldsymbol{H}^{-1}$, and $\Delta \boldsymbol{z}^n \in \boldsymbol{R}^n$ is corresponding to row n of the matrix $\Delta \boldsymbol{z}$.

The linear programming method is used to solve (12) and (13), and the corrections value $\Delta \underline{\boldsymbol{x}}$ and $\Delta \overline{\boldsymbol{x}}$ can be obtained. Thus, the second approximate solution of the upper/lower interval value of the state variable can be expressed as follows:

$$\begin{cases} \underline{\boldsymbol{x}}^{(l)} = \Delta \underline{\boldsymbol{x}} + \hat{\boldsymbol{x}}^{(l-1)} \\ \overline{\boldsymbol{x}}^{(l)} = \Delta \overline{\boldsymbol{x}} + \hat{\boldsymbol{x}}^{(l-1)} \end{cases} \tag{14}$$

If the interval value of state variable is expressed as $\left[\underline{x}^{(l)}, \overline{x}^{(l)}\right]$, then the given convergence criterion is as follows:

$$\max \begin{cases} \left|(\underline{V}_i)_k - (\underline{V}_i)_{k-1}\right| \\ \left|(\bar{V}_i)_k - (\bar{V}_i)_{k-1}\right| \\ \left|(\underline{\theta}_i)_k - (\underline{\theta}_i)_{k-1}\right| \\ \left|(\bar{\theta}_i)_k - (\bar{\theta}_i)_{k-1}\right| \end{cases} \le \varepsilon_1 \tag{15}$$

where k is the iteration number and ε_1 is the convergence criterion.

$\hat{x}^{(l)} = \frac{1}{2}(\overline{\boldsymbol{x}}^{(l)} + \underline{\boldsymbol{x}}^{(l)})$ instead of $\hat{\boldsymbol{x}}^{(l-1)}$ is used as the new initial value of the equation to solve the modified equation iteratively until the convergence criterion is reached and the feasible region of the state variable is obtained.

3.2 The Solving Method for the State Estimation Optimization Model

Substituting d_i into the objective function, the following results are obtained:

$$\begin{aligned} \min_x & \sum_{i=1}^{N} f\left(\frac{\boldsymbol{h}_i(\boldsymbol{x}) - \boldsymbol{z}_i}{U_i}\right) \\ \text{s.t.} \quad & \boldsymbol{g}(\boldsymbol{x}) = 0 \\ & \underline{\boldsymbol{x}} \le \boldsymbol{x} \le \overline{\boldsymbol{x}} \end{aligned} \tag{16}$$

By introducing the relaxation variables $\boldsymbol{s}_{xl}$ and $\boldsymbol{s}_{xu}$, the inequality constraints are transformed into equality constraints:

$$\begin{cases} \boldsymbol{x} - \boldsymbol{s_{xl}} - \underline{\boldsymbol{x}} = 0 \\ \boldsymbol{x} + \boldsymbol{s_{xu}} - \overline{\boldsymbol{x}} = 0 \\ \boldsymbol{s_{xl}} \ge 0 \\ \boldsymbol{s_{xu}} \ge 0 \end{cases} \tag{17}$$

Lagrange multiplier method is introduced, and augmented Lagrange function is constructed. The Lagrange multiplier method is used to solve the problem:

$$\begin{aligned} L = \boldsymbol{F}(\boldsymbol{x}) - \boldsymbol{y}^T \boldsymbol{g}(\boldsymbol{x}) - \boldsymbol{a}_{xl}^T(\boldsymbol{x} - \boldsymbol{s}_{xl} - \underline{\boldsymbol{x}}) - \boldsymbol{b}_{xu}^T(\boldsymbol{x} + \boldsymbol{s}_{xu} - \overline{\boldsymbol{x}}) \\ - \boldsymbol{\mu}\left[\sum_{j=1}^{m} \ln(\boldsymbol{s}_{xl(j)}) + \sum_{j=1}^{m} \ln(\boldsymbol{s}_{xu(j)})\right] \end{aligned} \tag{18}$$

where $F(\boldsymbol{x}) = \sum_{i=1}^{m} f\left(\frac{\boldsymbol{h}_i(\boldsymbol{x}) - \boldsymbol{z}_i}{\boldsymbol{U}_i}\right)$, μ is the disturbance factor; $\boldsymbol{y}$, $\boldsymbol{a}_{xl}$, and $\boldsymbol{b}_{xl}$ are Lagrangian multipliers. When the partial derivatives of L to variables and multipliers are 0, L can be taken as a minimum.

According to the KKT condition, the following relation can be obtained:

$$\nabla_{\boldsymbol{x}} L = \nabla \boldsymbol{F}(\boldsymbol{x}) - \nabla \boldsymbol{g}(\boldsymbol{x})^T \boldsymbol{y} - (\boldsymbol{a}_{xl} + \boldsymbol{b}_{xu}) = 0 \tag{19}$$

$$\nabla_{\boldsymbol{y}} L = \boldsymbol{g}(\boldsymbol{x}) = 0 \tag{20}$$

$$\nabla_{\boldsymbol{a}_{xl}} L = \boldsymbol{x} - \boldsymbol{s}_{xl} - \underline{\boldsymbol{x}} = 0 \tag{21}$$

$$\nabla_{\boldsymbol{b}_{xu}} L = \boldsymbol{x} + \boldsymbol{s}_{xu} - \overline{\boldsymbol{x}} = 0 \tag{22}$$

$$\nabla_{\boldsymbol{s}_{xl}} L = \boldsymbol{S}_{xl}\boldsymbol{A}_{xl}\boldsymbol{e} - \mu = 0 \tag{23}$$

$$\nabla_{\boldsymbol{s}_{xu}} L = \boldsymbol{S}_{xu}\boldsymbol{B}_{xu}\boldsymbol{e} - \mu = 0 \tag{24}$$

where $\boldsymbol{S}_{xl}$, $\boldsymbol{A}_{xl}$, $\boldsymbol{S}_{xu}$, and $\boldsymbol{B}_{xu}$ are diagonal matrices with $\boldsymbol{s}_{xl}$, $\boldsymbol{a}_{xl}$, $\boldsymbol{s}_{xu}$, and $\boldsymbol{b}_{xu}$ as diagonal elements, respectively; $\boldsymbol{e}$ is the unit column vector; and $\boldsymbol{\mu}$ is the column vector whose elements are all μ. When the relaxation factor $\boldsymbol{\mu}$ approaches zero, (16) and (18) have the same optimal solution. In the primal dual interior point method, the complementary gap G_{gap} and the centre parameter σ are used to make the relaxation factors $\boldsymbol{s}_{xl}$ and $\boldsymbol{s}_{xu}$ tend to zero

gradually. G_{gap} and the central parameter μ are defined as:

$$G_{gap} = \boldsymbol{a}_{xl}\boldsymbol{s}_{xl}^T - \boldsymbol{b}_{xu}\boldsymbol{s}_{xu}^T \tag{25}$$

$$\mu = \sigma \frac{G_{gap}}{k + 2m} \tag{26}$$

where $\sigma \in (0, 1)$ is called the central parameter. When it is generally taken as 0.1, the convergence effect of the state estimation is better.

Because of $\mu > 0$, $\underline{x} > 0$, $\bar{x} > 0$, it is known that $a_{xl} > 0$, $b_{xu} < 0$. Taking the complementary gap G_{gap} as the criterion of convergence, the criterion of convergence is reached when $G_{gap} < \varepsilon_2$, and finally the result of the state estimation is the output. Generally, $\varepsilon_2 = 10^{-6}$. The Newton–Raphson method is used to solve the problem.

4. The Studying Example

To test the feasibility and effectiveness of the proposed method, this paper compiles the test programme in Matlab environment and takes IEEE30 and IEEE118 systems as examples for analysis. The system parameters of IEEE30 and IEEE118 are in the appendix.

4.1 Impact of Data Selection

The IEEE30 system is selected as a study example. The measurement uncertainty $U_i = 3\sigma_i$, $k = 1.3$, $\lambda = 1.3333$, and centre parameter $\sigma = 0.8$ are set. The zero injection points are set for 6, 9, 22, 25, 27, and 28, respectively. The reference power is 1 MVA and the reference voltage is 12.66 kV. Unit value is used in the calculation.

In this paper, 2% Gaussian noise is added to the power flow calculation results of the IEEE30 system as measurement data. Bad data can be obtained by randomly adding or subtracting 20%, setting zero or changing symbols.

For the IEEE30 system, the actual physical numerical constraints, historical data constraints, and dynamic constraint of interval value constraints are used to analyse the examples, and the difference between the state estimation value and the true value is compared.

Three scenarios are set as follows:

1. Scenario 1: Based on the actual physical numerical constraints. For users of 35 kV and above, the allowable voltage deviation is −10 to 10% of the rated voltage. Therefore, the actual physical constraints are [0.945, 1.21]. The number of iterations of the state estimation based on the actual physical numerical constraints is 22. The estimated values of voltage amplitude and phase angle are, respectively, shown in Figs. 1 and 2. The change trend of the estimated value is consistent with the true value, and only a few points have large deviation from the true value. Based on the actual physical constraints, the solution range is relatively large. Obviously, from Figs. 1 and 2, it can be found that some nodes have large deviations between true and true values, and the accuracy of state estimates is low. Due to the large range of state variables, the accuracy of the state estimation is reduced to a certain extent. At the same time, the nodes with large voltage deviation and large phase angle deviation are load nodes. Due to the real-time dynamic changes of the load, the load measurement has caused a deviation and the accuracy of the state estimation is reduced.
2. Scenario 2: Constraints based on the historical data. Through the IEEE30 system, the change of load factor is adjusted to simulate the normal operation of the distribution network, and the voltage change range of each node is obtained. The change of voltage amplitude and phase angle is basically about ±5% of the true voltage value. Therefore, ±5% of the true voltage deviation is taken as the constraint of historical data. The number of iterations of the state estimation based on the historical data constraints is 8. The estimated values of voltage amplitude and phase angle are, respectively, shown in Figs. 3 and 4. The change trend of the estimated value is consistent with the true value, and the estimated value of the voltage phase angle basically coincides with the

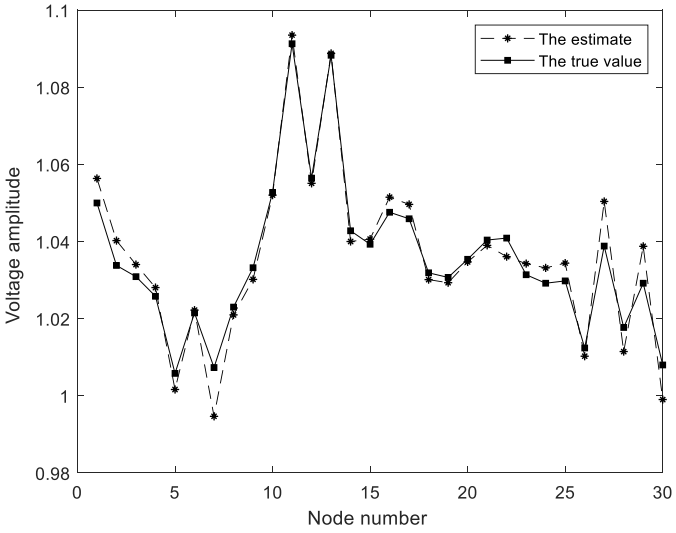

Figure 1. The state estimation values of voltage amplitude considering actual physical numerical constraints.

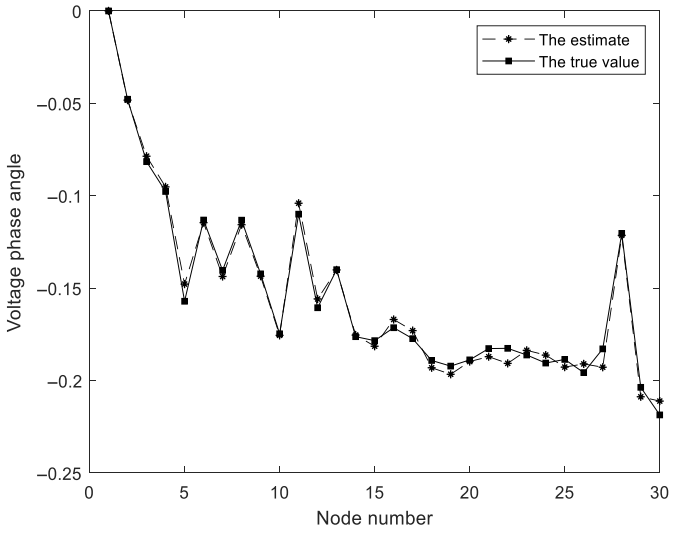

Figure 2. The state estimation values of voltage phase angle considering actual physical numerical constraints.

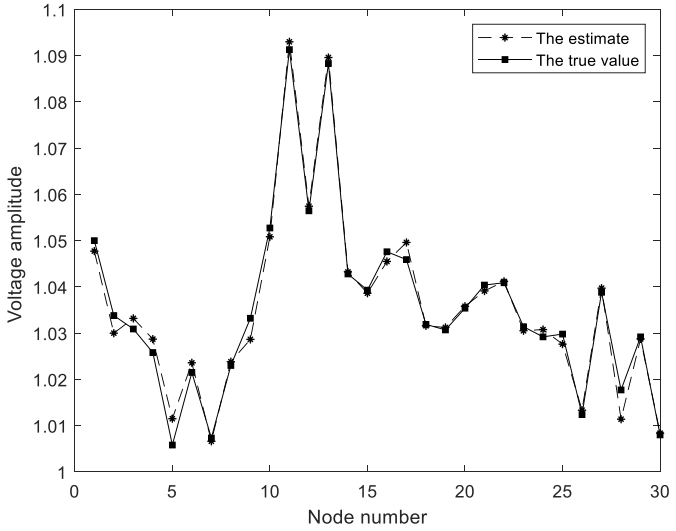

Figure 3. The state estimation values of voltage amplitude considering historical data constraints.

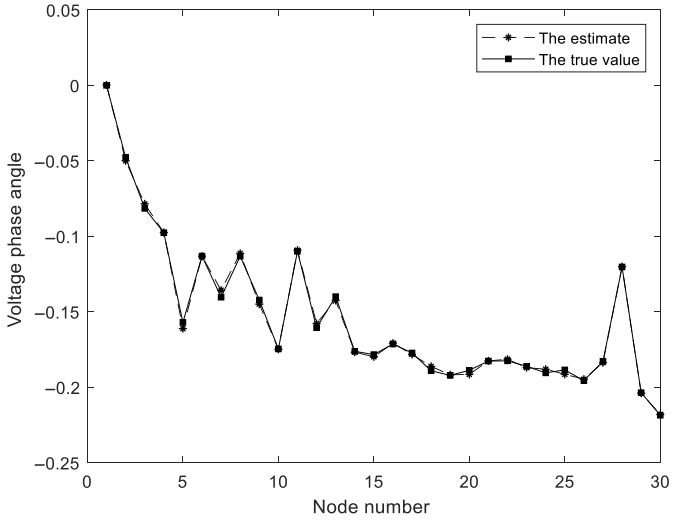

Figure 4. The state estimation values of voltage phase angle considering historical data constraints.

true value, but the voltage amplitude deviation is more obvious. Compared with the first scenario, under this constraint, the number of the state estimation solutions is reduced, and the deviation of voltage amplitude and phase angle is significantly smaller than scenario 1. The state estimation accuracy has been improved.

3. Scenario 3: Dynamic constraints based on the interval values. The interval values solved by the interval constraint model are shown in Figs. 5 and 6.

It can be seen that the results of the state estimation basically coincide with the true value, and the number of iterations is less than the first two scenarios, so the solution range of state variables is reduced, and the amount of calculation is reduced, so it has higher feasibility and effectiveness.

Compared with the first two constraints, they are both fixed and cannot express the feasible region of state variables well. By solving the interval of state variables,

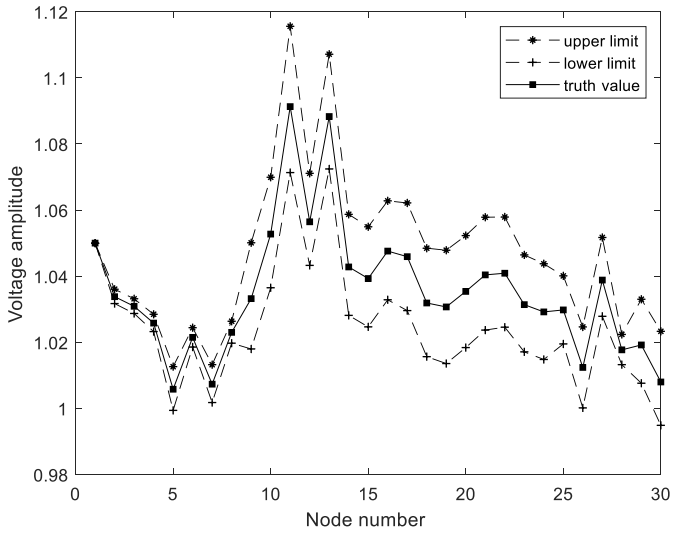

Figure 5. The upper and lower limits of voltage amplitude range constraint.

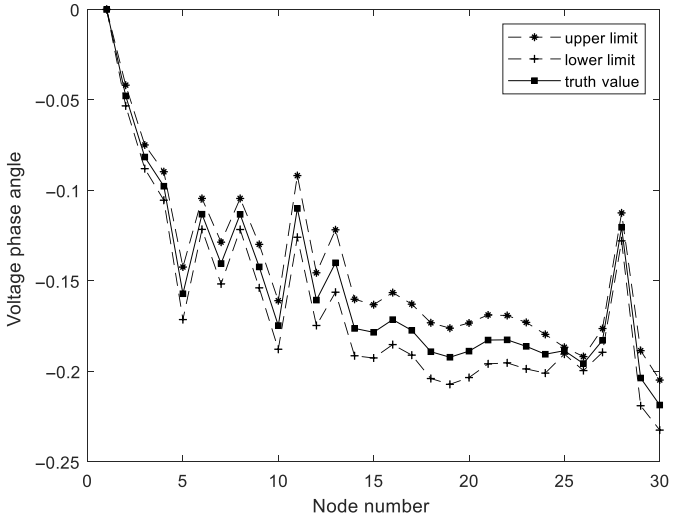

Figure 6. The upper and lower limits of voltage phase angle interval constraint.

the number of the state estimation solutions is reduced, and the accuracy of the state estimation is improved to a certain extent.

4.2 Estimation Accuracy Test

The relative deviation between the estimated value and the true value of the state variable is compared to characterize the estimation accuracy under the three constraints. The relative deviation indexes E_V and E_θ were defined as follows:

$$E_V = \frac{1}{n}\sum_{i=1}^{n}(V_i - \hat{V}_i)^2 \tag{27}$$

$$E_\theta = \frac{1}{n}\sum_{i=1}^{n}(\theta_i - \hat{\theta}_i)^2 \tag{28}$$

Table 1
State Accuracy Comparison Under Three Scenarios

System		IEEE30	IEEE118
Scenario 1	E_V	2.5339×10^{-5}	1.1192×10^{-6}
	E_θ	1.9893×10^{-5}	8.7034×10^{-7}
Scenario 2	E_V	5.8477×10^{-6}	1.0734×10^{-6}
	E_θ	5.7414×10^{-6}	8.4285×10^{-7}
Scenario 3	E_V	3.5156×10^{-8}	7.5986×10^{-7}
	E_θ	6.4916×10^{-8}	4.4612×10^{-7}

Table 2
Accurate Comparison of Measurements Under Three Scenarios

System		IEEE30	IEEE118
Scenario 1	E_p	5.1330×10^{-4}	1.4491×10^{-8}
	E_Q	2.0000×10^{-3}	1.9238×10^{-8}
Scenario 2	E_p	1.0839×10^{-5}	7.6589×10^{-9}
	E_Q	1.9109×10^{-6}	5.6676×10^{-9}
Scenario 3	E_p	3.5345×10^{-6}	9.2986×10^{-9}
	E_Q	3.5587×10^{-6}	1.1928×10^{-9}

where n is the number of nodes; V_i and θ_i are the state estimates of voltage amplitude and phase angle, respectively; and $\hat{V}_i$ and $\hat{\theta}_i$ are the true values of voltage amplitude and phase angle, respectively.

Table 1 shows the relative deviation index of the state estimation under different constraint scenarios for IEEE30 and IEEE118 systems. Obviously, the proposed method has better estimation accuracy. In the test, the voltage is per unit and the phase angle is in radian system.

The relative deviation of P_i and Q_i was used as evaluation index:

$$E_p = \frac{1}{m_p} \sum_{i=1}^{m_p} (P_i - \hat{P}_i)^2 \tag{29}$$

$$E_Q = \frac{1}{m_Q} \sum_{i=1}^{m_Q} (Q_i - \hat{Q}_i)^2 \tag{30}$$

where P_i and Q_i are the measured values of active power and reactive power injected into node i, respectively; $\hat{P}_i$ and $\hat{Q}_i$, respectively, calculate the active and reactive power values of node i using power flow calculation method; m_P and m_Q are the values measured by P_i and Q_i, respectively.

Table 2 shows the relative deviation indexes of the measured estimates obtained under different constraints of IEEE30 and IEEE118 systems. The relative measurement deviation of scenario 3 is smaller than that of the other two scenarios, which is more in line with the actual requirements.

Table 3
Comparison of the State Estimation Accuracy of the Two Methods Based on the Different Proportions of Bad Data

Ratio of	Method of this Paper		WLS	
Bad Data	E_V	E_θ	E_V	E_θ
0%	3.5156×10^{-8}	6.4916×10^{-8}	6.9779×10^{-5}	2.8702×10^{-5}
3%	4.5658×10^{-7}	9.6179×10^{-8}	2.1403×10^{-4}	6.1083×10^{-5}
6%	2.9781×10^{-5}	1.0392×10^{-5}	5.0100×10^{-2}	8.6700×10^{-2}

4.3 Method Comparison

The theoretical basis of traditional power system state estimation is the law of large numbers in traditional statistics, that is, when the number of measurements approaches infinity, the estimated value approaches the true value with a probability of 1. However, the number of quantitative measurements in the actual system is limited, sometimes even a small sample. At this time, the evaluation indicators and estimation accuracy of traditional state estimation are not theoretically guaranteed. At present, the most widely used state estimation method is the WLS estimation [20]. Its disadvantage is poor robustness and the estimation results are easily affected by bad measuring points. Based on the IEEE30 system, through two different estimation methods, under different proportions of bad data, the robustness and estimation accuracy of the two methods are compared. Bad data can be randomly selected. This paper simulates the bad data scenario by setting the data of V_6, V_{20}, P_{12}, P_{29}, Q_8, and Q_{15} to zero, changing the sign, and increasing or decreasing 20%.

From Table 3, it can be found that under normal circumstances, the method in this paper has better estimation ability and can obtain more accurate results. At a ratio of 3% of bad data, the estimation accuracy of the two methods decreases. At a ratio of 6% of bad data, the estimation accuracy decreases more obviously. Obviously, a high proportion of bad data seriously affects the accuracy of the state estimation results. As the proportion of bad data increases, the state estimation accuracy of the two methods has decreased, but the state estimation accuracy of WLS has decreased significantly. However, the method in this paper has high estimation accuracy, has good resistance to bad data, and guarantees that the state estimation result has better accuracy.

5. Conclusion

With the feasible region of state variables as constraints and the interval median as the initial value, it is unnecessary to take the power flow calculation results as the initial value, which can effectively reduce the solution range of state variables and reduce the amount of calculation.

Compared with the traditional method, this method has higher estimation accuracy and smaller relative deviation. Under normal circumstances, the measurement deviation can be guaranteed to be less than 10^{-5}, and the accuracy of the state estimation result can be guaranteed.

When there are different proportions of bad data, abnormal measurement points can be effectively identified, and the influence of bad data on the state estimation results can be reduced, which has good robustness. Through IEEE30 and IEEE118 node systems, simulation results verify the accuracy and robustness of the proposed method under normal operating conditions and bad data conditions.

Acknowledgement

This work was supported by Science and Technology Project of Guangzhou Power Supply Bureau of Guangdong Power Grid Co., Ltd. (GZHKJXM20190062).

References

[1] S.W. Fernandes, M.A. da Rosa, and D. Issicaba, A robust dynamic line rating monitoring system through state estimation and bad data analysis, *Electric Power Systems Research*, *189*, 2020, 106648.

[2] G.M. Hebling, J.A.D. Massignan, J.B.A. London Junior, & M.H.M. Camillo, Sparse and numerically stable implementation of a distribution system state estimation based on Multifrontal QR factorization, *Electric Power Systems Research*, 189, 2020, 106734.

[3] M. Schmidt and P. Schegner, Deriving power uncertainty intervals for low voltage grid state estimation using affine arithmetic, *Electric Power Systems Research*, *189*, 2020, 106703.

[4] K. Amiri and R. Kazemzadeh, Enhancement of two-step state estimation performance in unbalanced distribution networks, *Computers & Electrical Engineering*, *86*, 2020, 106724.

[5] H. Adjerid and A.R. Maouche, Multi-agent system-based decentralized state estimation method for active distribution networks, *Computers & Electrical Engineering*, *86*, 2020, 106652.

[6] P. Tatjewski and M. Ławryńczuk, Algorithms with state estimation in linear and nonlinear model predictive control. *Computers & Electrical Engineering*, *143*, 2020, 107065.

[7] T. Zhang, P. Yuan, Y. Du, W. Zhang, and J. Chen, Robust distributed state estimation of active distribution networks considering communication failures, *International Journal of Electrical Power & Energy Systems*, *118*, 2020, 105732.

[8] R. Brandalik and W.-H. Wellssow, Power system state estimation with extended power formulations, *International Journal of Electrical Power & Energy Systems*, *115*, 2020, 105443.

[9] Y. Chen, X. Kong, C. Yong, X. Ma, and L. Yu, Distributed state estimation for distribution network with phasor measurement units information, *Energy Procedia*, 158, 2019, 4129–4134.

[10] R. Džafić and R.A. Jabr, Real-time equality-constrained hybrid state estimation in complex variables, *International Journal of Electrical Power & Energy Systems*, *117*, 2020, 105634.

[11] G.-y. He, N.-c. Chang, S.-f. Dong, and B. Wang, Grid state identification based on set theory estimation (I) modeling. *Power System Automation*, *40*(05), 2016, 25–31.

[12] X. Kong, X. Zhang, C. Wang, P. Li, L. Yu, and X. Jiang, An adaptive self-optimization state estimation method for distribution networks in complex forms, *Chinese Journal of Electrical Engineering*, 2020, 1–10.

[13] J. He and L. Liu, Fast state estimation algorithm for intelligent distribution Networks in decoupled transformation mode. *Chinese Journal of Electrical Engineering*, *37*(04), 2017, 1088–1096.

[14] J. Xu, Z. Wu, Q. Hu, *et al.*, Trade-offs in meter deployment for distribution network state estimation considering measurement uncertainty, *IEEE Access*, *7*, 2019, 66123–66136.

[15] G. He and S. Dong, Power system state estimation based on measurement uncertainty (I) result evaluation, *Power System Automation*, *33*(19), 2009, 21–24+35.

[16] G. He and S. Dong, Power system state estimation based on measurement uncertainty (II) Method research, *Automation of Power Systems*, *33*(20), 2009, 32–36.

[17] Y. Zhang, J. Wang, and Z. Li, Interval state estimation with uncertainty of distributed generation and line parameters in unbalanced distribution systems, *IEEE Transactions on Power Systems*, *35*(1), 2020, 762–772.

[18] G. He and S. Dong, Comparison of power system State estimation algorithms based on measurement uncertainty, *Automation of Power Systems*, *33*(21), 2009, 28–31+71.

[19] A. Bahrami, S. Hosseinzadeh, R. Ghasemiasl, *et al.*, Solution of non-Fourier temperature field in a hollow sphere under harmonic boundary condition, *Applied Mechanics and Materials*, 2015, 772.

[20] Y. Zhang and J. Wang, Towards highly efficient state estimation with nonlinear measurements in distribution systems, *IEEE Transactions on Power Systems*, *35*(3), 2020, 2471–2474.

Biographies

Li Xin is with Guangzhou Power Supply Bureau of Guangdong Power Grid Co., Ltd. Guangdong, China. Her research topics lie at power system operation and control.

Wu Jiekang graduated from Zhejiang University. His special fields of interest included renewable power systems.

Zeng Shunqi is with Guangzhou Power Supply Bureau of Guangdong Power Grid Co., Ltd. Guangdong, China. His research topics lie at power system operation and control.

Cai Jinjian is with School of Automation, Guangdong University of Technology, Guangdong, China. His research topics lie at power system operation and control.